

Titania–silica hybrid films derived by a sol–gel process for organic field effect transistors

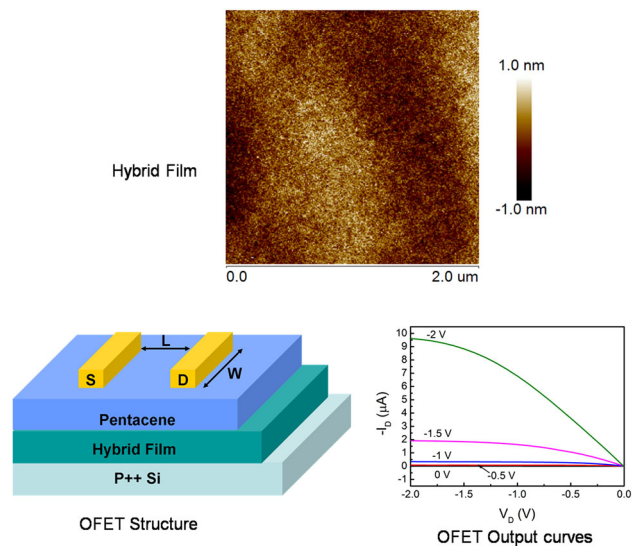
Jiaying Hu^{1,2} · Wenxiu Que¹  · Zhili Chen² · Jinyou Shao³

Received: 17 January 2017 / Accepted: 24 June 2017 / Published online: 6 July 2017
© Springer Science+Business Media, LLC 2017

Abstract Titania–silica hybrid films with a thickness of 300 nm are fabricated by combining a sol–gel method with a spin-coating process from the acid-catalyzed organically modified silane solution of γ -glycidoxypropyltrimethoxysilane, methyltriethoxysilane and tetrapropylorthotitanate. The dielectric constants of the titania–silica hybrid films can be easily controlled by adjusting titanium content. Effects of titanium content and heat treatment temperature on the leakage current and surface roughness of the as-fabricated films are also optimized, thus, the hybrid film with smooth surface ($R_q < 0.3$ nm), high dielectric constant ($k = 59.44$) and low leakage current density (< 1 nA cm⁻² at 5 V) is obtained and then used as the dielectric layer for the organic field effect transistors. Results indicate that the electrical properties of the organic field effect transistor fabricated by the titania–silica hybrid film as dielectric layer show an obvious improvement as compared with those of the organic field effect transistor fabricated by the thermally grown SiO₂ as dielectric layer, especially, in the improvement of the operating voltage (-2 V), field effect mobility (0.53 cm² V⁻¹ s⁻¹) and sub-threshold swing (~ 130 mV/dec). It can be concluded that the titania–silica hybrid film shows

a potential for the dielectric layer of the organic field effect transistors.

Graphical abstract



Keywords Titania–silica hybrid · Sol–gel method · Low voltage · Dielectric constant · Organic field effect transistors

✉ Wenxiu Que
wxque@mail.xjtu.edu.cn

¹ Electronic Materials Research Laboratory, International Center for Dielectric Research, Key Laboratory of the Ministry of Education, School of Electronic and Information Engineering, Xi'an Jiaotong University, Xi'an 710049 Shaanxi, People's Republic of China

² Micro-optoelectronic Systems Laboratories, Xi'an Technology University, Xi'an 710021 Shaanxi, People's Republic of China

³ State Key Laboratory for Manufacturing Systems Engineering, Xi'an Jiaotong University, Xi'an 710049 Shaanxi, People's Republic of China

1 Introduction

Organic field effect transistors (OFETs) have been attracting much attention because of low fabrication cost, light weight, flexibility, potential application, etc. [1–7]. In the past decades, OFETs have made a great progress in the field effect mobility, for example, the mobility of OFETs with

some organic semiconductor materials has exceeded several $\text{cm}^2 \text{V}^{-1} \text{S}^{-1}$ [8–11]. However, these devices still need much improvement for practical application due to high operating voltage. Two methods can be used to solve this problem. One way is to use ultra thin film as the dielectric [12, 13], but the ultra thin film is difficult to be fabricated and easy to be broken. Another way is to use high-k material as the dielectric, such as TiO_2 , Ta_2O_5 , Al_2O_3 , ZrO_2 and so on [14–18]. These materials have high permittivity, but as well have some defects including large leakage current and rough surface. So that they are often fabricated into bi-layer with other materials [19–21], thus, resulting in an increased hysteresis of the OFET. Recently, the hybrid film is becoming a new attractive dielectric layer in the OFETs [22, 23]. The hybrid films can be obtained by different methods [24–26], and their dielectric constants can be effectively improved by adjusting the titanium content. However, the leakage current and surface roughness of the hybrid films increase with an increasing titanium content. Actually, these defects hinder the application of the hybrid film in the transistors. Hence, it is crucial to obtain a hybrid film with low leakage current and smooth surface for OFETs.

Here, we reported a novel solution processed method for fabricating the TiO_2 - SiO_2 hybrid film from the acid-catalyzed organically modified silane solution of γ -glycidoxypolytrimethoxysilane (GLYMO), methyltriethoxysilane (MTES) and tetrapropylorthotitanate (TPOT). Effects of titanium content and heat treatment temperature on the structural and electrical properties of the hybrid films were also investigated and optimized. The as-prepared hybrid film exhibits smooth surface, low leakage current density and high permittivity, and the OFET fabricated from the optimized hybrid film as the dielectric layer achieves a low operating voltage, low sub-threshold swing (SS), low hysteresis and high on/off ratio.

2 Experimental

2.1 Titania-silicon hybrid film fabrication

The precursors for the titania-silicon hybrid films were prepared from the GLYMO ($[(\text{OCH}_2\text{CH})\text{CH}_2\text{OCH}_2\text{CH}_2\text{CH}_2\text{Si}(\text{OCH}_3)_3]$, Sigma Aldrich), MTES ($\text{CH}_3\text{Si}(\text{OC}_2\text{H}_5)_3$,

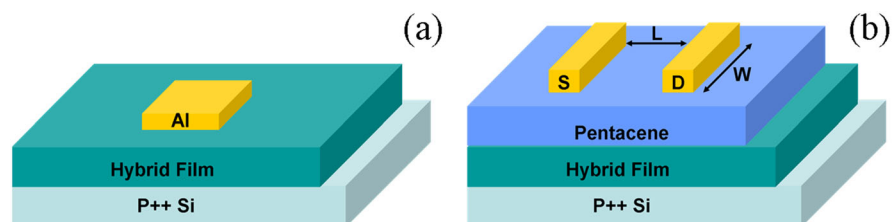
Sigma Aldrich) and TPOT ($\text{Ti}(\text{OC}_4\text{H}_9)_4$). Acetylaceton (Hacac) was used as a chelating agent of titanium alkoxide, hydrochloric acid (HCl, 37%) was used as a catalyst, and ethanol (EtOH) was used as a solvent. The precursor solutions of titania-silica hybrid films were synthesized by the following three solutions. For solution I, 1 mol MTES and 2 mol de-ionized water were mixed with 10 mol ethanol, and then 0.01 mol HCl was added into the solution. Then, the solution I was stirred for ten minutes. For solution II, 1 mol GLYMO and 2 mol de-ionized water were mixed with 10 mol ethanol, and the mixed solution was stirred for 10 min. For solution III, 1 mol TPOT was added into 4 mol Hacac, and the solution was also stirred for 10 min. Three solutions were then mixed at different molar ratios to adjust the titanium content. The final solution was stirred for 24 h at room temperature and filtrated through a 0.22- μm membrane before spin-coating. The p++ Si wafers were used as the substrates, which were ultrasonically cleaned in acetone, ethanol, de-ionized water, respectively, and dipped into dilute HF solution (HF: $\text{H}_2\text{O} = 1: 100$) to remove the native oxide. The hybrid films were deposited by spin-coating at 4000 rpm for 30 s in ambient environment. Finally, the deposited films were heated for 2 h at 100 °C, 200 °C, 500 °C and 1000 °C under the protection of argon, respectively. Thus, the dense, pinhole-free and transparent films could be obtained.

The hybrid films were characterized by Fourier transform infrared spectroscopy (FT-IR, Spectrum GX) and X-ray diffraction (XRD, Rigaku D/max 2400 \times). The surface morphological and cross-sectional properties of the hybrid films were observed by atomic force microscopy (AFM, Bruker Multimode 8) and scanning electron microscopy (SEM, JEOL JSM-6390), respectively. The thickness of the hybrid films was measured by optical profiler (Talysurf CCI 2000).

2.2 Metal-insulator-semiconductor (MIS) and OFET fabrication

MIS (Al/Film/p++ Si) structure was fabricated to analyze the gate leakage and the dielectric properties, as shown in Fig. 1a. In addition, the OFETs were also fabricated as shown in Fig. 1b. Here, the titania-silica hybrid film was used as the dielectric layer of the OFET. For comparison,

Fig. 1 Schematic illustration of **a** MIS structure and **b** a top-contacted OFET with the hybrid film



the thermally grown SiO_2 was also used as an insulation layer. Pentacene (Sigma Aldrich) without further purification was deposited onto the dielectric layer film. During the deposition of pentacene, the substrate temperature was kept at 50°C , the pressure of vacuum chamber was set as 5×10^{-4} Pa, the deposition rate was 0.5 \AA s^{-1} , which was monitored by a quartz crystal oscillator. The thickness of the pentacene film is 50 nm. Then, Au was deposited as the source/drain electrodes through a mask (channel length $L = 50 \text{ }\mu\text{m}$ and channel width $W = 5 \text{ mm}$). Thus, the as-obtained OFETs were tested in ambient conditions immediately after being fabricated. The capacitance of the MIS structure was measured by Agilent 4294A in 100 Hz frequency. The electrical characteristics of the OFETs were performed by using Keithley 4200 SCS.

3 Results and discussion

Figure 2a shows the FT-IR absorption spectra of the hybrid films with the molar ratio of $\text{Si}:\text{Ti} = 1:1$ at different heat treatment temperatures. The peak center at 1270 cm^{-1} is assigned to the symmetric deformation vibration of the $\text{Si}-\text{CH}_3$ bond and gradually decreases in intensity with the increase of the heat treatment temperature, and even disappears when the heat treatment temperature increases up to 500°C or above. The peak at 1100 cm^{-1} represents the asymmetric stretch of the $\text{Si}-\text{O}-\text{C}$ bond [27]. This peak in

intensity gradually decreases with increasing heat treatment temperature and vanishes when the heat treatment temperature reaches 1000°C . The peak center at 1080 cm^{-1} is the asymmetric stretch vibration of the $\text{Si}-\text{O}-\text{Si}$ bond. This peak starts to appear at 500°C and becomes very obvious at 1000°C . The peaks at 1100 cm^{-1} , 1080 cm^{-1} , and 1270 cm^{-1} show that the organic groups of the hybrid films gradually disappear with the increase of the heat treatment temperature, and only inorganic parts are left in the film when the heat treatment temperature increases up to 1000°C . The peak at 615 cm^{-1} represents the stretch vibration of the $\text{Ti}-\text{O}$ bond. This peak in intensity changes little as the heat treatment temperature increases. The peak at 430 cm^{-1} is mainly caused by the $\text{Si}-\text{O}$ bond and its intensity increases a lot as the heat treatment temperature reaches at 1000°C . Figure 2b shows the FT-IR absorption spectra of the films with different titanium contents and heated at 1000°C . The peak at 955 cm^{-1} is associated with the stretch vibration of the $\text{Si}-\text{O}-\text{Ti}$ bond, which is weak and decreases in intensity as the titanium content increases. The peaks at 1080 cm^{-1} and 430 cm^{-1} decrease in intensity, while the peak at 615 cm^{-1} in intensity shows a little increase as the titanium content increases. It can be concluded from above results that the film obtained at the heat treatment temperature of 1000°C is composed of silica and titania.

Figure 3a shows that the hybrid film obtained from the $\text{Si}:\text{Ti} = 1:1$ is amorphous when the heat treatment

Fig. 2 FT-IR absorption spectra of the hybrid films **a** with the molar ratio of $\text{Si}:\text{Ti} = 1:1$ at different heat treatment temperatures and **b** with different titanium contents and heated at 1000°C

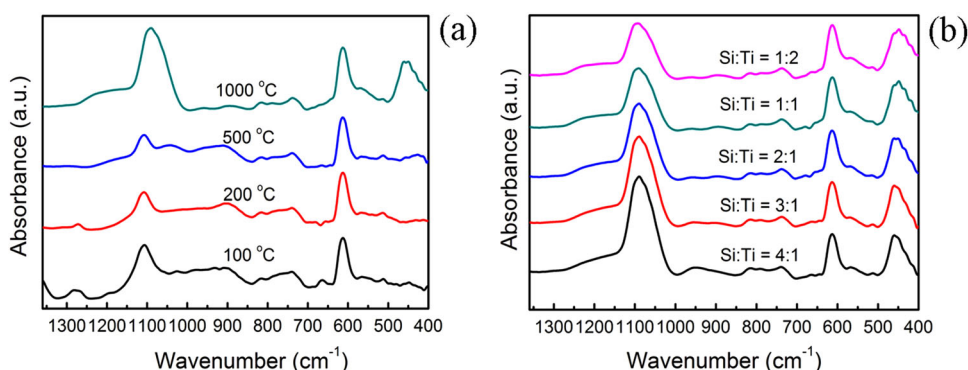


Fig. 3 XRD patterns of the hybrid films **a** with the molar ratio of $\text{Si}:\text{Ti} = 1:1$ at different heat treatment temperatures and **b** with different titanium contents and heated at 1000°C

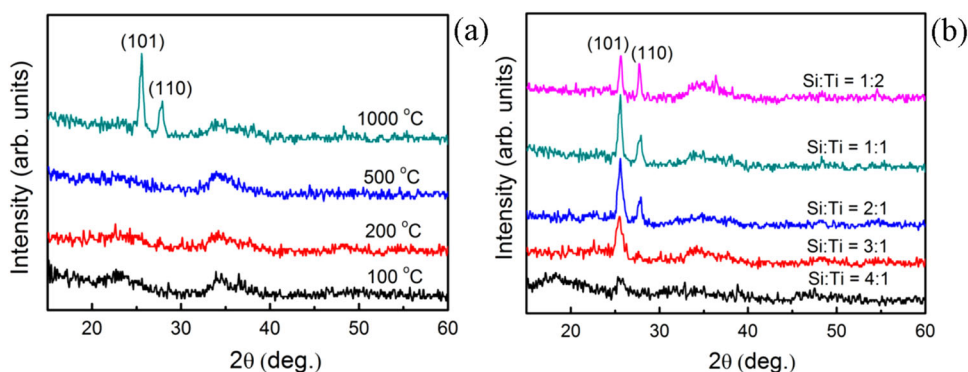


Fig. 4 AFM surface images of the hybrid films with the molar ratio of Si:Ti = 1:1 at **a** 100 °C, **b** 200 °C, **c** 500 °C and **d** 1000 °C

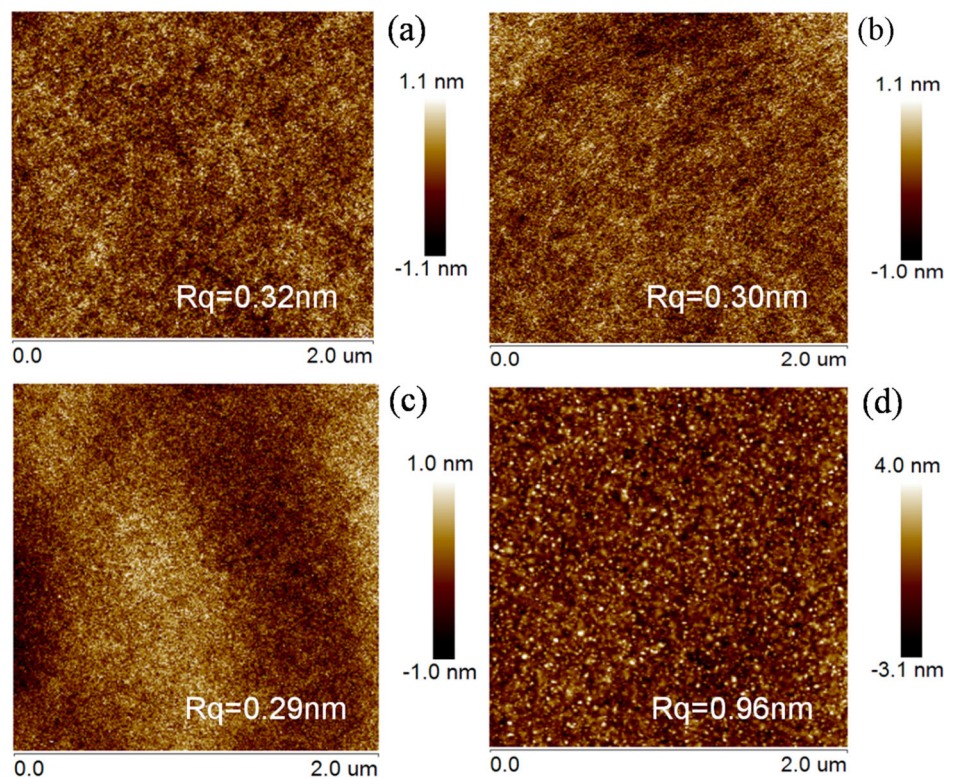
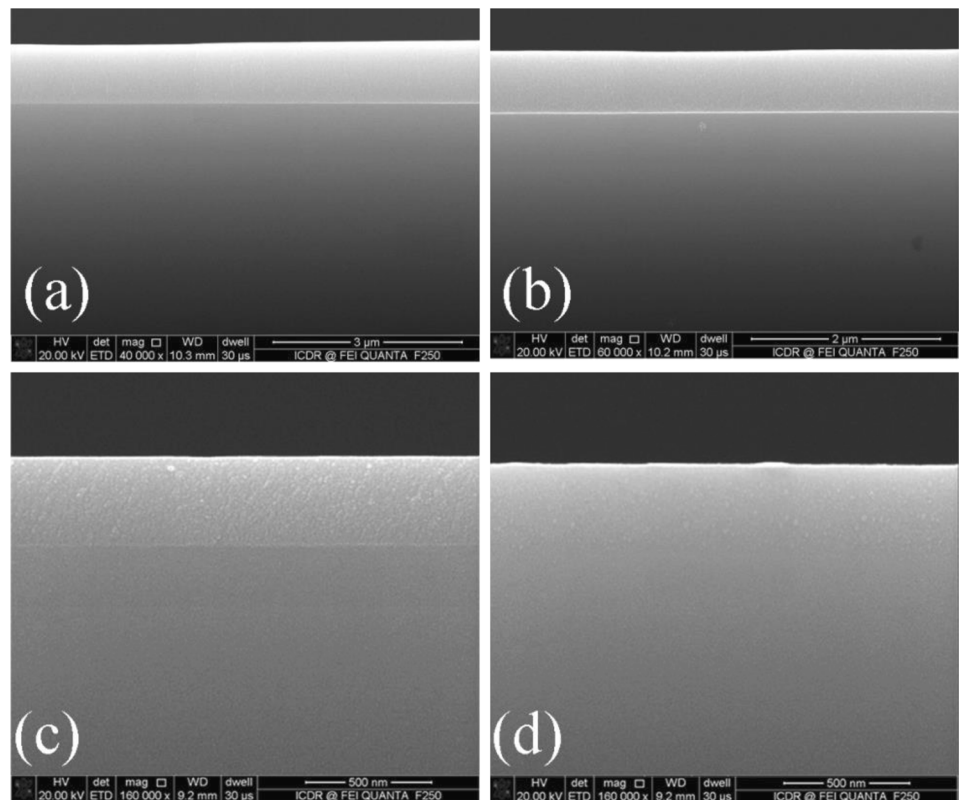


Fig. 5 Cross-section SEM images of the hybrid films with the molar ratio of Si:Ti = 1:1 at **a** 100 °C, **b** 200 °C, **c** 500 °C and **d** 1000 °C



temperature is below or equal to 500 °C. The diffraction peak at 25.28° corresponds to the (101) plane of the anatase phase and the peak at 27.45° corresponds to the (110) plane

of the rutile phase of titania, indicating that the film heated at 1000 °C contains anatase and rutile crystalline phases. Figure 3b shows the XRD patterns of the films with

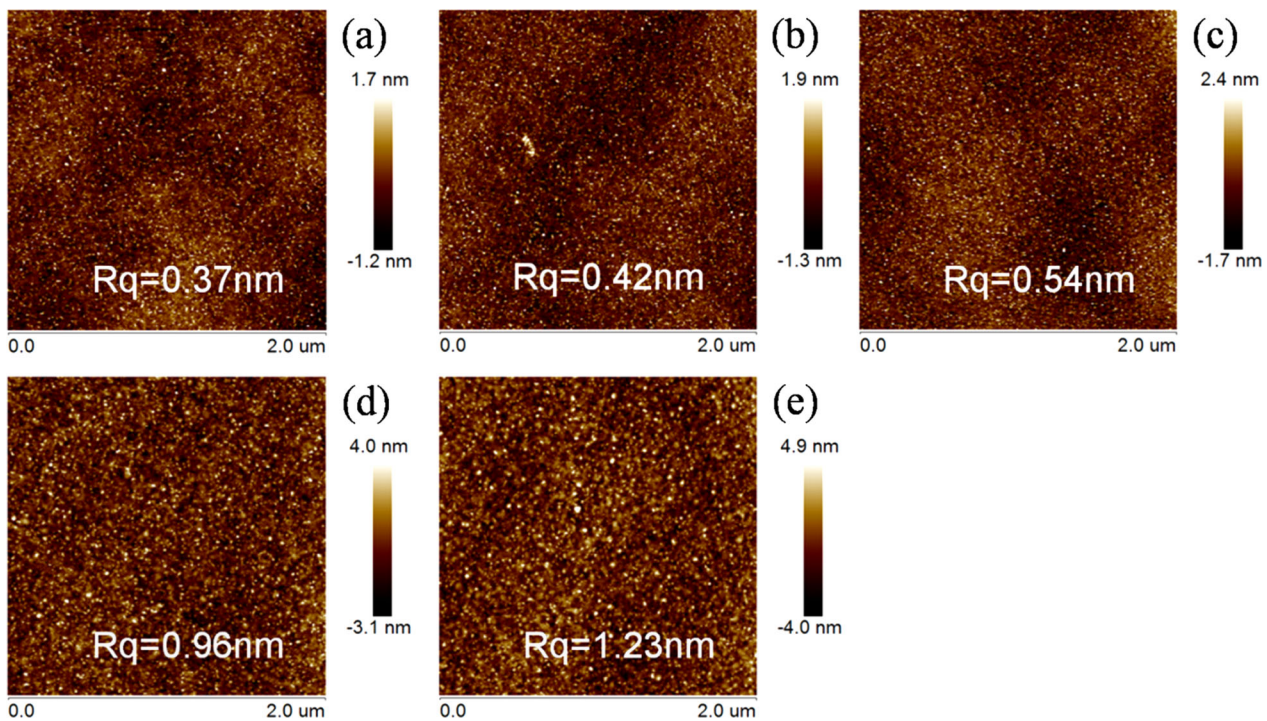


Fig. 6 AFM images of the films heated at 1000 °C with different titanium contents: **a** Si:Ti = 4:1, **b** Si:Ti = 3:1, **c** Si:Ti = 2:1, **d** Si:Ti = 1:1 and **e** Si:Ti = 1:2

different titanium contents and heated at 1000 °C. It can be seen that when the molar ratio of silicon and titanium is 4:1, the film shows only a weak anatase phase. As the titanium content increases, the anatase crystalline phase becomes obvious and the rutile crystalline phase begins to appear. The rutile phase in the film becomes more obvious, while the anatase crystalline phase in the film starts to weaken as the titanium content increases further. It can be concluded from FI-IR and XRD results that the hybrid film is amorphous when the heat treatment temperature is below 500 °C. When the heat treatment temperature increases up to 1000 °C and the titanium content is low, the film shows only a weak anatase phase. As the titanium content increases, the rutile crystalline phase starts to appear and becomes obvious, while the anatase crystalline phase weakens gradually.

Figure 4 shows the AFM surface morphologies of the films derived from the molar ratio of Si:Ti = 1:1 and heated at different temperatures. The root-mean-square surface roughness (R_q) of the films are below 0.4 nm when the heat treatment temperature is below 500 °C, while the R_q of the film increases to 0.96 nm as the heat treatment temperature increases to 1000 °C. The surface roughness value of the film heated at 1000 °C becomes bigger due to the crystallization of the film. Figure 5 shows the cross-section SEM images of the films derived from the molar ratio of Si:Ti = 1:1 and heated at different temperatures. It can be observed that the grains are isolated in the film when the heat

Table 1 Thickness and dielectric constants at low-frequency (100 Hz) of the hybrid films with the molar ratio of Si:Ti = 1:1 and at different heat treatment temperatures

Temperature (°C)	100	200	500	1000
Thickness (nm)	916	646	305	280
Dielectric constant	4.29	3.95	59.44	9.47

treatment temperature increases to 1000 °C and the film becomes thinner as the heat treatment temperature increases. Figure 6 shows the AFM images of the films with different titanium contents and heated at 1000 °C; it can be clearly observed that the crystalline grains become more and more obvious with the increase of the titanium content, which leads to the increase of the R_q of the films. The surfaces of all films obtained at different conditions show pinhole-free morphologies as shown in Figs. 4 and 6. It can be also seen from Table 1 that the thickness of the films decreases as the heat treatment temperature increases. Table 1 also shows dielectric constants at low-frequency (100 Hz) of the hybrid films with the molar ratio of Si:Ti = 1:1 at different heat treatment temperatures. The permittivity of the film heated at 200 °C is less than that of the film baked at 100 °C, it is probably related to that the combustion of the organic groups leads to the porosity inside the films [28, 29]. The dielectric constant of the film increases up to 59.44 when the heat temperature increases to 500 °C, it should be attributed to the dense and inorganic film.

However, the dielectric constant reduces to 9.47 when the heat treatment temperature further increases to 1000 °C. FTIR results indicate that the Si–O bonds become more obvious as the heat treatment temperature increases to 1000 °C, and the surface of silicon wafer may be oxidized at such high temperature, as a result, the silica content of the film increases and thus the permittivity of the film decreases. These analyzes can be further confirmed by the cross-section SEM images of the films as shown in Fig. 5, where obvious interface between the film and the substrate can be observed when the heat treatment temperature is at 100 °C, 200 °C, and 500 °C. However, the interface between the film and the substrate becomes indistinct as the heat treatment temperature increases to 1000 °C, which can infer that the wafer surface should be oxidized. Table 2 shows that the dielectric constants of the films increase with the increasing of titanium content.

Figure 7a shows the relationship of the leakage current density versus bias voltage of the films derived from the molar ratio of Si:Ti = 1:1 and heated at different temperatures. The leakage current density of the film baked at 100 °C is less than 1 nA cm⁻² under the bias voltage of 30 V, because the film baked at this temperature is dense and thicker, and thus a low porosity. The leakage current density of the film heated at 200 °C increases rapidly, which should be related to the high porosity of the film, this is because that the organic groups of the film start to decompose at such a higher temperature, and thus the film easily absorbs water molecules in ambient. However, the leakage current density of the film heated at 500 °C is far lower than that of the film heated at 200 °C due to dense inorganic film. The film heated at 1000 °C shows well

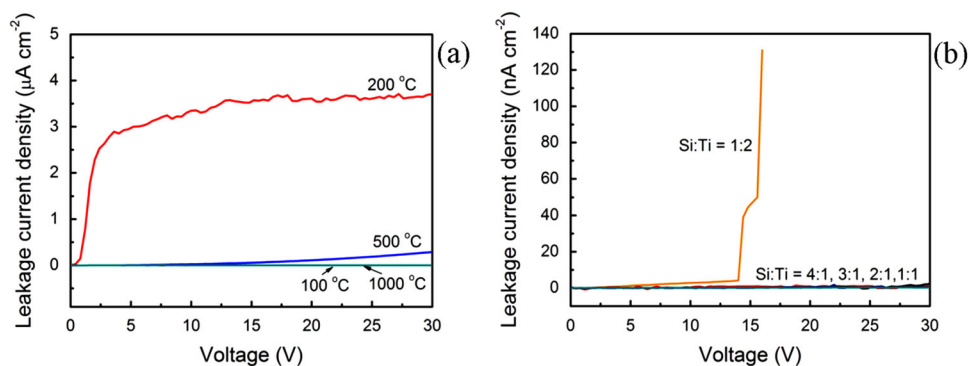
insulation property and thus its leakage current density is less than 1 nA cm⁻² at 30 V, which should be attributed to the possible oxidization of the wafer surface and dense inorganic film due to so high heat treatment temperature. Figure 7b shows the leakage current density of the titania–silica hybrid films with the same thickness about 300 nm. It can be seen that these films, which the molar ratios of Si:Ti are 4:1, 3:1, 2:1, and 1:1, show an excellent insulation property. However, for the film derived from the molar ration of Si:Ti = 1:2, the leakage current density increases and the breakdown voltage decreases.

The operating voltage of OFET can be reduced by increasing the gate capacitance and the surface roughness of the gate dielectric is also particularly important for hindering the movement of charge carriers. Hence, the titania–silica films derived from the molar ratio of Si:Ti = 1:1 and heated at 500 °C and 1000 °C were used as the dielectric layer of the OFET, and named GMT500 and GMT1000, respectively. The thicknesses of the films are both 300 nm, which can be obtained by controlling the spin-coating speed. The dielectric constants at low-frequency (100 Hz) of the GMT500 and GMT1000 are 59.44 and 9.47, and the capacitance values at low-frequency of the GMT500 and GMT1000 are 162 and 22 nF m⁻², respectively. The R_q values of these films are 0.29 nm and 0.96 nm, respectively. The leakage current density of the GMT500 is less than 1 nA cm⁻² when the bias voltage is 5 V, and that of the GMT1000 is 30 V. The OFET with thermally grown SiO₂ (thickness: 300 nm, R_q: 0.28 nm) film as dielectric layer was also fabricated as a reference device. The grain size of the pentacene on the dielectric layer is an important factor to affect the mobility of the OFET. Figure 8 shows the surface topography images of the vacuum deposited pentacene grown on SiO₂, GMT500 and GMT1000 films. It can be observed that there are two types of pentacene grains on the GMT500 film, including large grains and small grains. The average size of large grains is 1 μm, which is smaller than the size (1.5 μm) of the grains grown on the SiO₂ film, while the average size of small grains is only 300 nm. There are only small pentacene

Table 2 Dielectric constants at low-frequency (100 Hz) of the films (thickness: 300 nm) with different titanium contents and heated at 1000 °C

Molar ratio of Si: Ti	4: 1	3: 1	2: 1	1: 1	1: 2
Dielectric constant	5.97	6.32	7.83	9.47	12.98

Fig. 7 Leakage current density versus bias voltage of the hybrid films **a** with the molar ratio of Si:Ti = 1:1 at different heat treatment temperatures and **b** with different titanium contents (thickness: 300 nm) and heated at 1000 °C



grains on the GMT1000 film. Therefore, the titania-silica hybrid film needs surface modification to get well grown pentacene film.

Figure 9 shows the output and transfer curves of the as-fabricated organic transistors. A high saturation current ($9.5 \mu\text{A}$) at $V_g = -2\text{V}$ has been observed in the OFET with

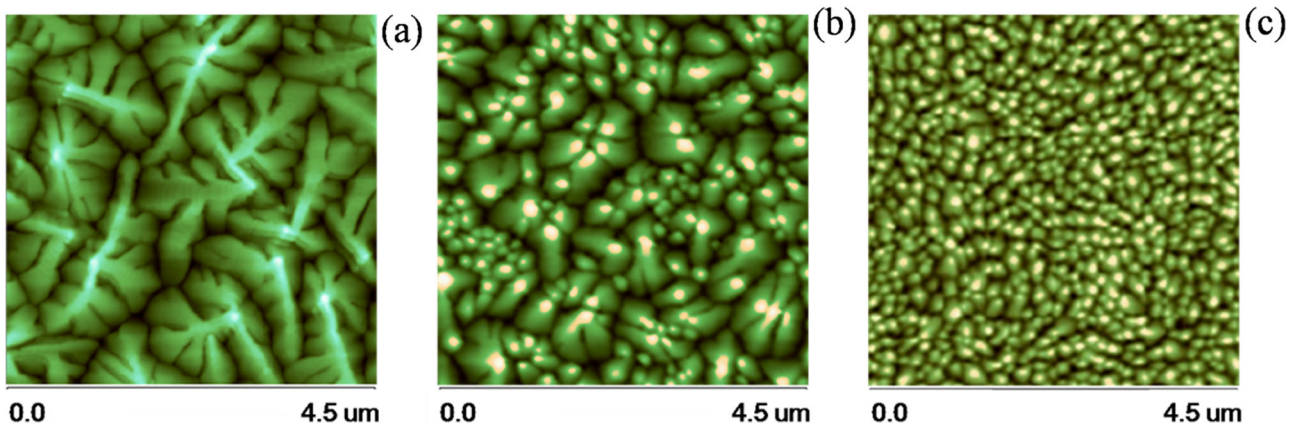


Fig. 8 AFM images of pentacene films grown on **a** SiO_2 , **b** GMT500 and **c** GMT1000

Fig. 9 **a** Output curves and **b** Transfer curves of the OFETs fabricated from SiO_2 as the dielectric layer, **c** Output curves and **d** Transfer curves of the OFETs fabricated from GMT500 as the dielectric layer, **e** Output curves and **f** Transfer curves of the OFETs fabricated from GMT1000 as the dielectric layer

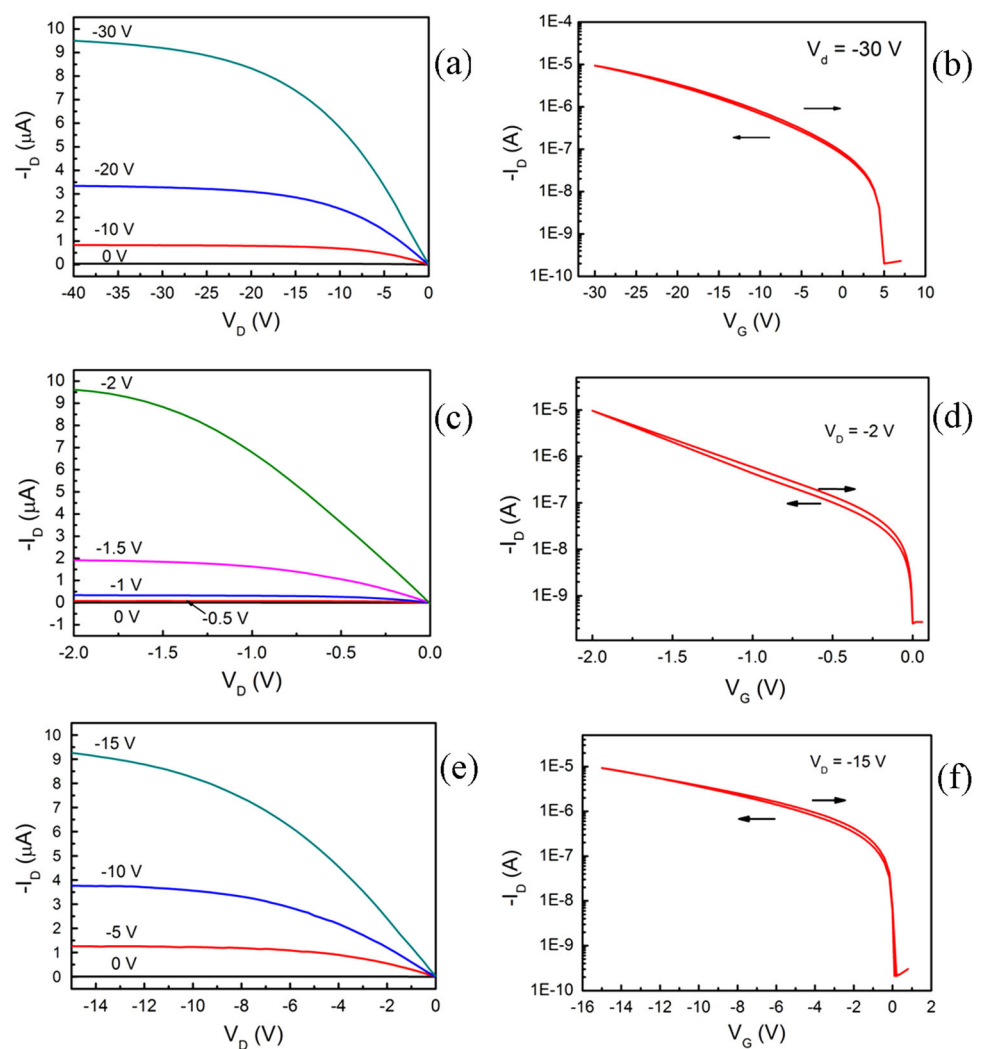


Table 3 Electrical performances of the OFETs fabricated from the hybrid film and thermally grown SiO₂ film, respectively

Electric properties	μ_{FET} (cm ² V ⁻¹ s ⁻¹)	V_{th} (V)	SS (mV dec ⁻¹)	On/off ratio
SiO ₂	0.06 ± 0.01	-4.9	680	1 × 10 ⁴
GMT500	0.53 ± 0.05	-0.4	130	1 × 10 ³
GMT1000	0.08 ± 0.02	-1.9	160	1 × 10 ⁴

GMT500 gate dielectric, and high $V_{\text{g}} = -15\text{V}$ and -30V are required to obtain similar current for the OFETs with GMT1000 and SiO₂ gate dielectric, respectively. In order to calculate the field-effect mobility and threshold voltage, the following formula was used

$$I_{\text{DS}} = \frac{W}{2L} C_i \mu_{\text{FET}} (V_{\text{g}} - V_{\text{th}})^2$$

where W and L are the channel width and length, μ_{FET} is the field-effect mobility, C_i is the capacitance of the insulation, V_{th} is the threshold voltage and V_{g} is the gate voltage. The electrical performances of all as-fabricated OFETs are summarized in Table 3. In the previous studies, there are two contradictory views with the μ_{FET} of OFETs: a μ_{FET} increased or decreased as the dielectric constant increased [30, 31]. Although the R_{q} values of GMT500 (0.29 nm) and SiO₂ (0.28 nm) are very close and the average size of pentacene grains on GMT500 film is smaller than that on SiO₂ film as mentioned above, the mobility of OFET fabricated from GMT500 film (0.53 cm² V⁻¹ s⁻¹) is much larger than that of OFET fabricated from SiO₂ film (0.07 cm² V⁻¹ s⁻¹). We think that the high mobility of OFET based on GMT500 is mainly contributed to its high dielectric constant. The high dielectric constant increases the gate capacitance, inducing more free carriers into the channel to enhance the mobility of the devices. The threshold voltage of the device from GMT500 is -0.4V , which is much lower than that of the OFET from SiO₂ (-4.9V). The SS is a very important parameter for determining the voltage swing required for a transistor to turn from “off” to “on”, and should be as low as possible. The SS of the OFET fabricated from the GMT500 is low to 130 mV dec⁻¹ in ambient conditions. The low SS is helpful for improving switching speed. The OFET with GMT1000 has low mobility (0.08 cm² V⁻¹ s⁻¹) and large threshold voltage (-1.9V). Actually, high surface roughness of GMT1000 ($R_{\text{q}} = 0.96\text{nm}$) film forms trap states at organic/dielectric interface, and the large number of trap states at interface increases the threshold voltage and decreases the mobility of the device. The small size of pentacene grains is another reason for low mobility. In addition, the OFET fabricated from GMT500 film also has small hysteresis as seen in Fig. 8b, which is close to the device fabricated from the thermally grown SiO₂ film.

4 Conclusions

The titania–silica hybrid films with smooth, pinhole-free, low leakage current and high permittivity have been successfully fabricated by the sol–gel method. At the heat treatment temperature of 1000 °C, the organic groups of the hybrid film are completely removed and thus the titania–silica inorganic film is formed. The leakage current density of the titania–silica film is very small ($<1\text{ nA cm}^{-2}$) at the bias voltage of 30 V and the permittivity decreases due to the oxidization of the wafer surface at such high temperature. The surface roughness of the hybrid films increases with the increasing of the titanium content, and the R_{q} of the films derived from the molar ratio of silicon and titanium = 1:1 is less than 0.3 nm when the heat treatment temperature is 500 °C. When the molar ratio of silicon and titanium is larger than 1:1, the leakage current of the film increases and the breakdown voltage reduces as the heat treatment temperature increases. Furthermore, the as-prepared hybrid films were used as the dielectric layer of the OFETs, and the as-fabricated OFETs show low SS, low off-current and relatively low threshold voltage. Compared to the OFET fabricated from the thermally grown SiO₂, the mobility, threshold voltage and SS are obviously improved. Present work shows that the as-prepared titania–silica hybrid films are an excellent potential material as the insulation layer for the OFETs.

Acknowledgements This work was funded by the Research Fund for the Doctoral Program of Higher Education of China under Grant 20120201130004, the Science and Technology Developing Project of Shaanxi Province under Grant No. 2015KW-001, partially by the National Natural Science Foundation of China Major Research Plan on Nanomanufacturing under Grant No. 91323303, and the 111 Project of China (B14040). The SEM work was done at the International Center for Dielectric Research, Xi'an Jiaotong University, Xi'an, P. R. China, and the AFM work was done at the Micro-optoelectronic Systems Laboratories, Xi'an Technology University, P. R. China.

Compliance with ethical standards

Conflict of interest The authors declare that they have no competing interests.

References

1. Sekitani T, Zschieschang U, Klauk U, Someya T (2010) Flexible organic transistors and circuits with extreme bending stability. *Nat Mater* 9:1015–1022. doi:10.1038/NMAT2896
2. Abe Y, Dai T, Manaka T, Iwamoto M (2014) Study of carrier transport in flexible organic field-effect transistors: analysis of bending effect and microscopic observation using electric-field-induced optical second-harmonic generation. *Thin Solid Films* 554:166–169. doi:10.1016/j.tsf.2013.05.160
3. Baeg KJ, Khim D, Kim J, Han H (2012) Controlled charge transport by polymer blend dielectrics in topgate organic field-

- effect transistors for low-voltage-operating complementary circuits. *ACS Appl Mater Interfaces* 4:6176–6184. doi:10.1021/AM301793m
4. Gelinck G, Heremans P, Nomoto K, Anthopoulos TD (2010) Organic transistors in optical displays and microelectronic applications. *Adv Mater* 22:3778–3798. doi:10.1002/adma.200903559
 5. Kim YJ, Lee HS, Noh JS (2016) Transient behaviors of ZnO thin films on a transparent, flexible polyethylene terephthalate substrate. *Thin Solid Films* 603:160–164. doi:10.1016/j.tsf.2016.02.012
 6. Han S, Zhuang X, Shi W, Yang X, Li L (2016) Poly(3-hexylthiophene)/polystyrene (P3HT/PS) blends based organic field-effect transistor ammonia gas sensor. *Sens Actuators B Chem* 225:10–15. doi:10.1016/j.snb.2015.11.005
 7. Wang Y-F, Tsai M-R, Lin Y-S, Wu F-C, Lin C-Y (2015) High-response organic thin-film memory transistors based on dipole-functional polymer electret layers. *Org Electron* 26:359–364. doi:10.1016/j.orgel.2015.08.006
 8. Facchetti A (2007) Semiconductors for organic transistors. *Mater Today* 10:28–37. doi:10.1016/s1369-7021(07)70017-2
 9. Yamashita Y (2009) Organic semiconductors for organic field-effect transistors. *Sci Technol Adv Mater* 10:024313. doi:10.1088/1468-6996/10/2/024313
 10. Oniwa K, Kikuchi H, Shimotani H, Ikeda S, Asao N, Yamamoto Y (2016) 2-Positional pyrene end-capped oligothiophenes for high performance organic field effect transistors. *Chem Commun* 52:4800–4803. doi:10.1039/c6cc00948d
 11. Wang Y, Zou S, Gao J, Zhang H, Lai G, Yang C (2015) High-performance organic field-effect transistors based on single-crystalline microribbons of a two-dimensional fused heteroarene semiconductor. *Chem Commun* 51:11961–11963. doi:10.1039/c5cc03305e
 12. Hutchins DO, Acton O, Weidner T, Cernetic N, Baio JE, Castner DG (2012) Solid-state densification of spun-cast self-assembled monolayers for use in ultra-thin hybrid dielectrics. *Appl Surf Sci* 261:908–915. doi:10.1016/j.apsusc.2012.09.013
 13. Ono S, Häusermann R, Chiba D, Shimamura K, Ono T (2014) High performance organic field-effect transistors with ultra-thin HfO₂ gate insulator deposited directly onto the organic semiconductor. *Appl Phys Lett* 104:013307. doi:10.1063/1.4860998
 14. Majewski LA, Schroeder R, Grell M (2005) One volt organic transistor. *Adv Mater* 17:192–196. doi:10.1002/adma.200400809
 15. Deman AL, Tardy J (2005) PMMA-Ta₂O₅ bilayer gate dielectric for low operating voltage organic FETs. *Org Electron* 6:78–84. doi:10.1016/j.orgel.2005.03.002
 16. Hwang DK, Fuentes-Hernandez C, Kim JB, Potscavage WJ, Kippelen B (2011) Flexible and stable solution-processed organic field-effect transistors. *Org Electron* 12:1108–1113. doi:10.1016/j.orgel.2011.04.002
 17. Liao M, Ishiwarara H, Ohmi SI (2014) Excellent current drivability and environmental stability in room-temperature-fabricated pentacene-based organic field-effect transistors with HfO₂ gate insulators. *IEEE Trans Electron Devices* 61:569–575. doi:10.1109/ted.2013.2292904
 18. Hasan M, Nguyen MC, Kim H, You SW, Jeon YS, Tong DT (2015) High performance solution processed zirconium oxide gate dielectric appropriate for low temperature device application. *Thin Solid Films* 589:90–94. doi:10.1016/j.tsf.2015.04.035
 19. Su YR, Xie WG, Li Y, Shi Y, Zhao N, Xu JB (2013) A low-temperature, solution-processed high-k dielectric for low-voltage, high-performance organic field-effect transistors (OFETs). *J Phys D Appl Phys* 46:095105. doi:10.1088/0022-3727/46/9/095105
 20. Su Y, Wang C, Xie W, Xie F, Chen J, Zhao N, Xu J (2011) Low-voltage organic field-effect transistors (OFETs) with solution-processed metal-oxide as gate dielectric. *ACS Appl Mater Interfaces* 3:4662–4667. doi:10.1021/am201078v
 21. Gedda M, Subbarao NVV, Obaidulla SM, Goswami DK (2013) High carrier mobility of CoPc wires based field-effect transistors using bi-layer gate dielectric. *AIP Adv* 3:112123. doi:10.1063/1.4834355
 22. Han S, Zhuang X, Shi W, Yang X, Li L, Yu J (2016) Poly(3-hexylthiophene)/polystyrene (P3HT/PS) blends based organic field-effect transistor ammonia gas sensor. *Sens Actuators B Chem* 225:10–15. doi:10.1016/j.snb.2015.11.005
 23. Bahari A, Shahbazi M (2016) Electrical properties of PVP-SiO₂-TMSPM hybrid thin films as ofet gate dielectric. *J Electron Mater* 45:1201–1209. doi:10.1007/s11664-015-4262-y
 24. Busani T, Devine RAB, Yu X, Seo HW (2006) Electrical and physical properties of room temperature deposited, mixed TiO₂/SiO₂ oxides. *J Vac Sci Technol* 24:369–374. doi:10.1116/1.2172951
 25. Benito N, Palacio C (2014) Mixed Ti–O–Si oxide films formation by oxidation of titanium–silicon interfaces. *Appl Surf Sci* 301:436–441. doi:10.1016/j.apsusc.2014.02.094
 26. Peng J, Sheng C, Shi J, Li X, Zhang J (2014) High-k titanium–aluminum oxide dielectric films prepared by inorganic–organic hybrid solution. *J Solgel Sci Technol* 71:458–463. doi:10.1007/s10971-014-3400-y
 27. Hacker CA, Anderson KA, Richter LJ, Richter CA (2005) Comparison of Si–O–C interfacial bonding of alcohols and aldehydes on Si(111) formed from dilute solution with ultraviolet irradiation. *Langmuir* 21:882–889. doi:10.1021/la048841x
 28. Yu S, Wong TKS, Hu X, Pita K, Ligatchev V (2004) Synthesis and characterization of templating low dielectric constant organosilicate films. *J Electrochem Soc* 151:F123–F127. doi:10.1149/1.1688800
 29. Que W, Hu X (2003) Influence of titanium content and temperature on optical and mechanical properties of sol-gel derived TiO₂/γ-glycidoxypropyltrimethoxysilane and methyltrimethoxysilane hybrid organic-inorganic films. *J Phys D Appl Phys* 36:908–914
 30. Tan HS, Mathews N, Cahyadi T, Zhu FR, Mhaisalkar SG (2009) The effect of dielectric constant on device mobilities of high-performance, flexible organic field effect transistors. *Appl Phys Lett* 94:263303. doi:10.1063/1.3168523
 31. Ortiz RP, Facchetti A, Marks TJ (2009) High-k organic, inorganic and hybrid dielectrics for low-voltage organic field-effect transistors. *Chem Rev* 110:205–239. doi:10.1021/cr9001275